Title

Immunocytochemical localization of the neural-specific regulatory subunit of the type II cyclic AMP-dependent protein kinase to postsynaptic structures in the rat brain.

Journal

Brain research, 520(1-2)

ISSN

0006-8993

Authors

Ludvig, N
Ribak, CE
Scott, JD
et al.

Publication Date

1990-06-01

DOI

10.1016/0006-8993(90)91694-c

Brain Research, 520 (1990) 90–102
Elsevier

BRES 15591

Immunocytochemical localization of the neural-specific regulatory subunit of the type II cyclic AMP-dependent protein kinase to postsynaptic structures in the rat brain

Nandor Ludvig[1], Charles E. Ribak[1], John D. Scott[2] and Charles S. Rubin[3]

[1]*Departments of Anatomy and Neurobiology,* [2]*Physiology and Biophysics, University of California, Irvine, CA 92717 (U.S.A.) and* [3]*Department of Molecular Pharmacology, Albert Einstein College of Medicine, Bronx, NY 10461 (U.S.A.)*

(Accepted 12 December 1989)

Key words: Immunocytochemistry; Electron microscopy; Cyclic adenosine monophosphate; Protein kinase; Regulatory subunit; Postsynaptic site

The cellular and subcellular distribution of a major cyclic AMP binding protein in the central nervous system, the neural-specific regulatory subunit of the type II cyclic AMP-dependent protein kinase (RII-B), was analyzed in rat brains with light and electron microscopic immunocytochemical methods. The distribution of the non-neural isoform of the regulatory subunit of the enzyme (RII-H) was also analyzed. It was found that RII-B immunoreactivity was predominantly localized to neurons whereas glial and endothelial cells were unlabeled. In the neurons the RII-B immunoreactivity occurred in the perikaryal cytoplasm and in the dendrites; there was no significant accumulation of immunoreaction product in nuclei, myelinated axons and axon terminals. Although immunoreactivity was never detected in axon terminals, it was characteristically associated with the postsynaptic densities and the surrounding non-synaptic sites in somata, dendrites and dendritic spines. The localization of RII-B antigenic sites did not show specificity to any type of neuron or synapse, but the amount of immunoreactivity varied. The distribution of RII-H immunoreactivity was similar to that of RII-B except that RII-H immunoreaction product was also observed in glial cells and occurred more frequently in myelinated axons. Our data confirm that RII-B is one of the major cyclic AMP binding proteins in neurons, and provide morphological support for the involvement of the type II cyclic AMP-dependent protein kinase in postsynaptic neural functions.

INTRODUCTION

Second messenger systems, such as the cyclic AMP (cAMP) system, play an important, though not completely understood role in the regulation of synaptic transmission in the central nervous system[22,23]. Indeed, extracellular application of membrane-permeant analogues of cAMP affects the synaptic excitability in vitro[13,20] and can induce marked behavioral and electrographic effects in vivo[8,18,19]. Although some electrophysiological data show that cAMP can act directly on ion channels[12], the only known receptor proteins that mediate the effects of cAMP in the brain are the regulatory subunits of the cAMP-dependent protein kinases (cAMPdPK)[17,34]. It has also been shown that two major categories of cAMP binding proteins exist: RI and RII, the regulatory subunits of the type I and type II cAMPdPK, respectively[22,23].

Since the brain contains significantly more of the type II cAMPdPK than the type I kinase[2,34] and specific destruction of neurons by intracerebral injection of kainic acid depleted selectively the type II cAMPdPK[35], RII seems to be a major candidate for mediating the effects of cAMP in neurons in the central nervous system. In addition, Erlichman et al. found that RII in the brain was immunologically distinct from the form present in skeletal muscle, liver, kidney and heart[6]. Further biochemical studies have confirmed that there are two subclasses of RII: a neural-specific and a non-neural isoform, RII-B and RII-H, respectively[33]. RII-B and RII-H are the products of related but distinct genes[32,36]. Consequently, clarifying the functions of RII-B in synaptic processes is necessary for understanding the role of the cAMP signal transduction system in the brain.

An immunocytochemical analysis of the cellular and subcellular distribution of RII can provide important data for understanding the role of cAMPdPK. To date, only the non-neural isoform has been examined with immunocytochemical methods in the brain. It was shown that RII-H immunoreactivity occurs in both neuronal and glial elements[3,5]. The intensity of RII-H staining varied from cell to cell but within a stained neuron it was concentrated in the dendrites and perikaryon[4,5]. Subcellularly, RII-H seems to be accumulated on microtubules, micro-

Correspondence: N. Ludvig, Department of Basic Sciences, University of Illinois, College of Medicine at Peoria, Peoria, IL 61656, U.S.A.

tubule-organizing centers and in the area of the Golgi complex[5]. Its presence within the nucleus was unclear, because positive and negative immunostaining were both reported depending on whether unfixed[3] or fixed [5] tissue preparations were used.

In the present study we have demonstrated the cellular and subcellular distribution of RII-B immunoreactivity in rat brains with light and electron microscopic methods. We also examined the distribution of RII-H immunoreactivity to determine whether any differences exist in the localization of these cAMP binding proteins.

MATERIALS AND METHODS

A total of 20 adult Sprague–Dawley rats (180–240 g), both males and females, were used in this study. A part of the animals (n = 14) was utilized for methodological tests to determine the optimal immunocytochemical procedure for revealing the specific RII-B or RII-H tissue antigens. The following parameters were analyzed: (1) staining pattern in both fixed and unfixed tissue; (2) staining intensity after the use of different fixatives; (3) staining pattern in both frozen and non-frozen tissue; and (4) signal-to-noise ratio following both overnight and 1-h incubation with the primary antibody. Subsequent to these tests, experiments were conducted on 6 rats with the procedure that provided optimal results. Details on this latter method are given in light and electron microscopic immunocytochemistry sections.

Antibodies

The RII-B antibody used in this study was prepared and characterized, as described previously[6,33]. Briefly, the RII-B subunits were purified from bovine cerebral cortex by a combination of ion exchange chromatography on DEAE-cellulose and affinity chromatography on 8-(6-aminohexyl) amino-cAMP-Sepharose 4B. The antisera to highly purified RII-B were prepared in New Zealand white rabbits. Specificity to obtained antisera against RII-B was determined by: (1) indirect immunoprecipitation; (2) competitive displacement radioimmunoassay; and (3) Western immunoblot analysis.

The RII-H antibody was prepared and characterized, as follows. Peptide P13 (Ile-Val-Ser-Pro-Thr-Thr-Phe-His-Thr-Gln-Glu-Ser-Ser), representing residues 35–48 of the murine RII-H[29], was synthesized on an Advanced Biosystems Ab 430 solid-phase peptide synthesizer as previously described[28]. Cleavage from the resin was achieved by incubation in 75% HF/25% anisole for 30 min at 0 °C. The amount and composition of the peptide was determined by amino acid analysis using Waters Picotag system, and amino acid sequence analysis of P13 was performed on a Beckman 890C liquid-phase peptide sequinator. Peptide P13 was covalently coupled to the carrier protein rabbit serum albumin using carbodiimide. The antiserum was prepared in New Zealand white rabbits. A high titer of antiserum was obtained, and 10 ng of RII-H was detected with an antiserum dilution of 1:1000. No immunoreactivity toward RII-H was detected with the preimmune serum.

Tissue preparation

The rats were anesthetized (ketamine, 70 mg/kg–xylazine, 6 mg/kg; i.p.) and transcardially perfused with 100 ml of 0.1 M phosphate buffered saline (PBS), pH = 7.4, followed by 450 ml of freshly prepared paraformaldehyde (4%) and glutaraldehyde (0.1%) in PBS. The brains were removed and cut into 3 mm-thick blocks which were postfixed in 1% paraformaldehyde overnight. Coronal sections (40 μm) were cut with a vibratome, and they were collected in PBS and processed for either light or electron microscopic immunocytochemistry. Thus, adjacent sections from the same specimen could be analyzed at both light microscopic and ultrastructural levels. These analyses focused on the following areas: cerebral cortex, hippocampus, thalamus and the midbrain including the inferior colliculus.

Light microscopic immunocytochemistry

The sections were transferred onto gelatin-coated glass-slides on which the immunocytochemical procedure was conducted. Each section was framed by a thin Plexiglas ring (1.8 mm diameter) that was sealed with G-S hypo-tube cement (Germanow-Simon Corporation). The ring surrounded the entire section to form a barrier so that only a small amount of incubation fluid (450 μl) was required for each step per section. The immunostaining procedure involved the following incubation steps: (1) 20% normal goat serum and 0.25% Triton X-100; 30 min; (2) 1:500 dilution of RII-B or RII-H antibody and 2% normal goat serum; 60 min; (3) 1:200 dilution of biotinylated anti-rabbit IgG; 60 min; (4) 1% avidin: biotinylated horseradish peroxidase complex; 60 min; and (5) 0.05% diaminobenzidine and 0.01% H_2O_2; 4 min. Each step was separated from each other by a 15-min wash in PBS and all the solutions were made up in PBS. The slides were dehydrated through a series of alcohol solutions and coverslipped after removal of the rings by a razor blade. They were then viewed with a light microscope and examined with a MCID computerized image analysis system (Imaging Research, Inc.).

Electron microscopic immunocytochemistry

The staining procedure for electron microscopic immunocytochemistry was the same as that for the light microscopic studies except that free-floating sections were incubated. The immunostained specimens were dehydrated in ethanol and embedded in Epon 812. Serial thin sections were cut on a Sorvall ultramicrotome in the silver interference color range. The thin sections were mounted on formvar-coated slot grids, counterstained with lead citrate and uranyl acetate and examined with the electron microscope.

Control immunocytochemistry

In each experiment control studies were run parallel to the RII-B and RII-H immunocytochemistry to determine whether any artifacts were superimposed on the specific staining. In these studies, the primary antibodies were replaced with non-immune rabbit serum. Otherwise all the procedures were the same as described above. In addition, Nissl staining was used for some adjacent sections to determine the proportion of cellular elements labeled with the primary antisera.

RESULTS

The methodological tests showed that the use of fixative was essential to obtain information about the cellular and subcellular distribution of RII-B. Although immunoreaction product occurred in unfixed tissue processed for RII-B immunocytochemistry, cellular elements were almost unrecognizable. However, the general staining pattern was not significantly affected by using relatively mild (4% paraformaldehyde) or stronger (4% paraformaldehyde–0.2% glutaraldehyde) fixation. Similarly, the distribution of RII-B was basically identical in both frozen and unfrozen tissue. Free-floating and slide-mounted sections displayed the same staining. Surprisingly the factor that profoundly affected the immunocytochemical results was the incubation time with the primary antibody. It was found that long (overnight) incubation with either primary antibodies resulted in

artifacts and consequently a low signal-to-noise ratio, as compared to sections that were incubated for a short, 1-h period. This shorter incubation period decreased significantly the amount of artifactual immunoreactivity (Fig. 1) and thus a high signal-to-noise ratio was obtained with this method.

Light microscopic observations

Sections incubated with RII-B antibody displayed specific immunostaining in all of the brain regions examined. For example, all layers of the cerebral cortex displayed immunoreaction product except for the underlying white matter (Fig. 1B). The amount of immunostaining for RII-B in the white matter was at a similar level as that found throughout the control sections incubated with non-immune serum (Fig. 1). The staining intensity for RII-B, as it was determined by computerized image analysis, was higher in the cerebral cortex, hippocampus, and thalamus than in the midbrain including the inferior colliculus, indicating that the regional distribution of RII-B was not homogeneous. It is interesting to note that in the hippocampus the immunoreaction product was more concentrated in the dendritic layers than in the cellular layers (Fig. 4A).

At higher magnification, the RII-B immunostaining was observed in many neurons in each brain region. As predicted from the lack of immunostaining in the white matter, myelinated axons and glial cells did not appear to display RII-B immunostaining. The blood vessels of the neuropil also did not seem to contain specific immunoreactivity. In all of the brain regions examined, a consistent finding was that RII-B immunoreactivity was localized to the perikaryal cytoplasm and the proximal dendritic processes of the neurons (Fig. 2). The neuronal nuclei were always negative for RII-B staining (Figs. 2 and 3). The staining pattern did not seem to be specific

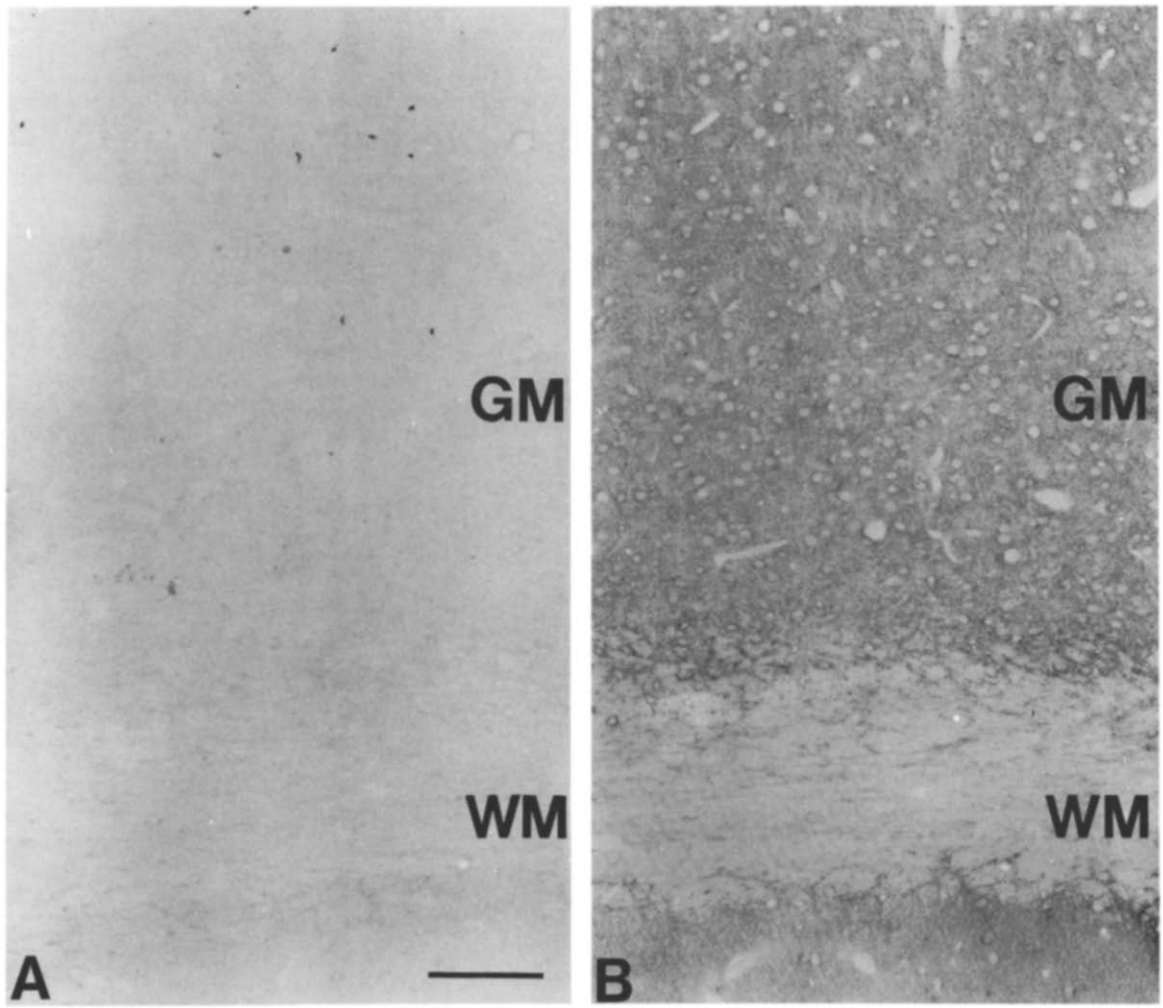

Fig. 1. Photomicrographs of two adjacent coronal sections through the parietal cortex incubated with either non-immune rabbit serum (A) or RII-B antiserum (B). Aside from a few red blood cells, the section incubated in non-immune serum (A) lacks staining in both the gray (GM) and white matter (WM). In contrast the section incubated in RII-B antiserum (B) displays immunoreaction product in the gray matter (GM) whereas the white matter (WM) lacks immunoreactivity. Scale bar for A and B = 100 μm.

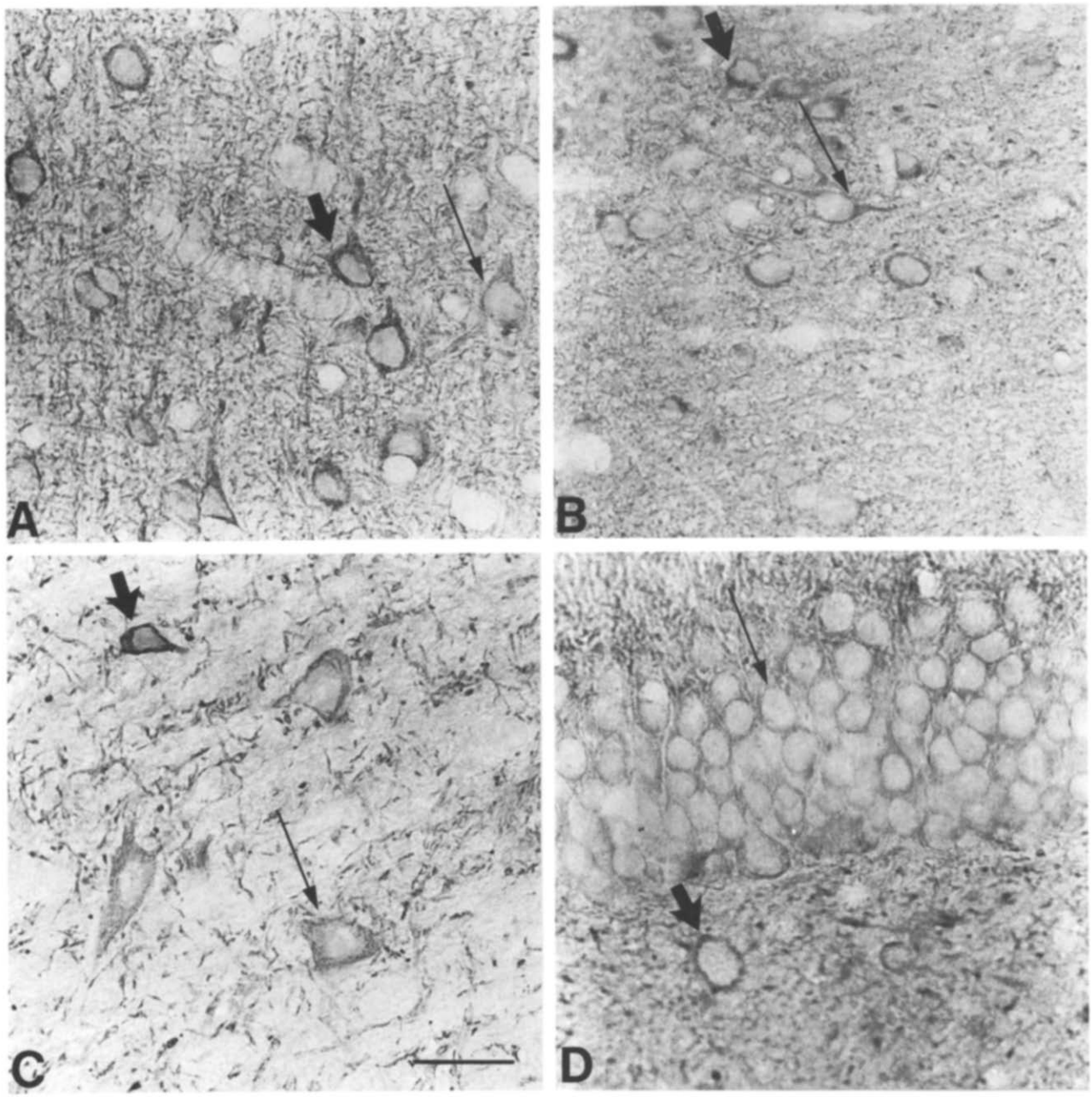

Fig. 2. Photomicrographs of RII-B immunostained sections from the same rat showing layer III of the parietal cortex (A), posterior thalamic nuclear group (B), central nucleus of the inferior colliculus (C) and suprapyramidal blade of the dentate gyrus (D). The immunostaining is prominent within neuronal somata (arrows) and their proximal dendrites, and is also found within small processes in the neuropil. Note the variation of the amount of immunoreaction product distributed in the labeled neurons; both strongly (thick arrows) and lightly (thin arrows) labeled cells are present in the same section. In the dentate gyrus (D), for example, the granule cells (thin arrow) are less densely immunostained than a hilar neuron (thick arrow). Scale bar for A–D = 25 μm.

for any particular neuron type. In the cerebral cortex both pyramidal and non-pyramidal (e.g. bipolar)[25] neurons were stained (Fig. 2A). In the thalamus RII-B staining was detected in the characteristic, scattered small neurons[7] and in some medium-size, multipolar neurons of the posterior nuclear group (Fig. 2B). In the inferior colliculus the medium-size, round GABAergic neurons[27] and the large, disc-shaped non-GABAergic neurons both displayed RII-B immunoreactivity (Fig. 2C). In the hippocampal formation all neuronal types were immunostained, including the granule cells, the basket cells and the hilar neurons of the dentate gyrus[1,31] (Fig. 2D) and the pyramidal cells of the CA1 (Fig. 3B) and CA3 regions (Fig. 4A). Most dendrites of these cells were uniformly labeled except for the CA3 pyramidal cells that displayed more dense immunostaining in the dendritic

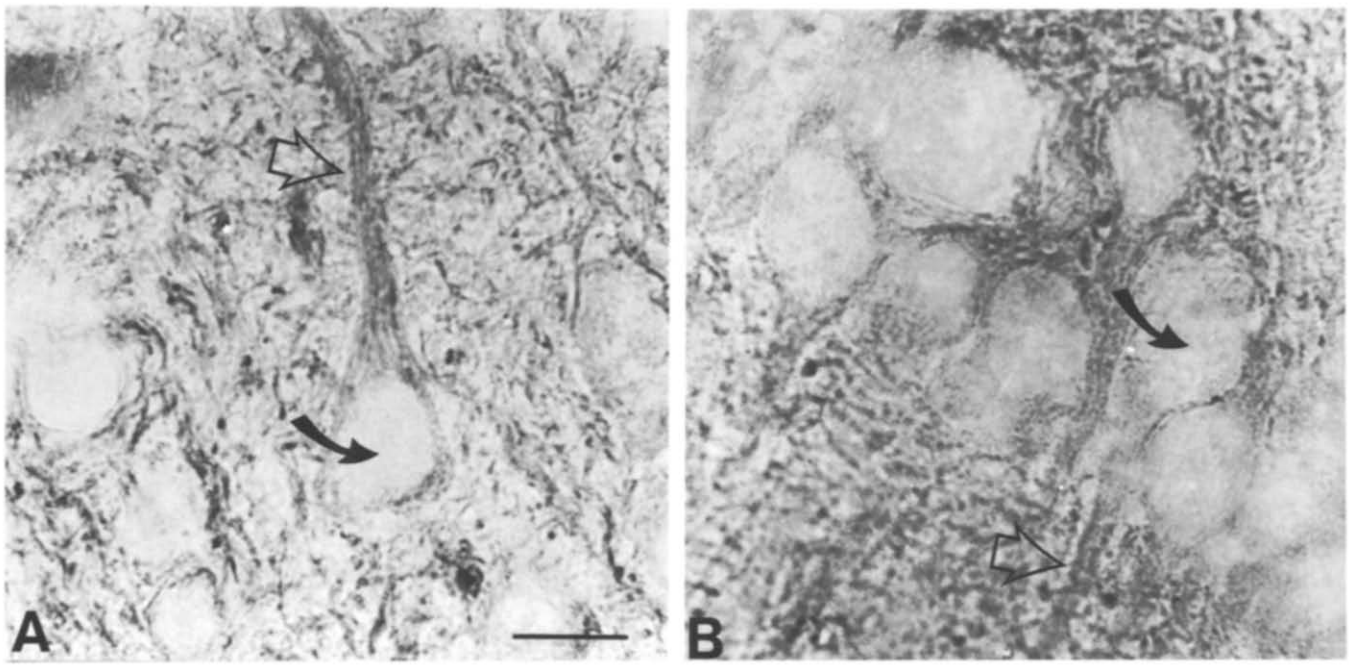

Fig. 3. Photomicrographs of RII-B immunostained sections from layer III of parietal cortex (A) and CA1 region of the hippocampus (B). The immunostaining is concentrated in the proximal apical dendrites (open arrows), whereas the neuronal nuclei (curved arrows) lack immunoreaction product. Scale bar for A and B = 10 μm.

portions found in the stratum lucidum.

The regional distribution of RII-H immunoreactivity was similar to that of RII-B. However, in certain areas such as the hippocampus, differences were observed: the stratum lucidum of CA3 region displayed more dense RII-B than RII-H immunostaining (Fig. 4). As in the case of RII-B staining, the RII-H immunoreaction product occurred predominantly in neurons. It should be noted, however, that cellular profiles resembling astrocytes revealed by glutamate dehydrogenase histochemistry[16] were often observed in RII-H-stained sections, although these glial elements were much less densely labeled than the neurons.

Electron microscopic observations

At the ultrastructural level the RII-B immunoreactivity was exclusively found to be associated with neuronal elements; no evidence could be detected for the presence of RII-B antigenic sites in glial cells. As was predicted from the light microscopic results, RII-B immunoreaction product was accumulated throughout the neuronal somata, whereas the nuclei, including the nuclear envelopes, and the nucleoli displayed no immunoreactivity (Figs. 5 and 7B). The immunoreaction product in the somata was evenly distributed in the perikaryal cytoplasm. However, the overall staining intensity varied from soma to soma. For example, the somata of the large pyramidal cells of layer V of the parietal cortex were markedly more densely stained than that of the granule cells of the dentate gyrus (Figs. 5 and 7). It should be noted that neurons negative for RII-B immunoreactivity were also found in the analyzed brain regions. The immunoreaction product was not preferentially associated with any organelles in the perikarya because it was localized to cisternae of the granular endoplasmic reticulum, Golgi complex, microtubules and the outer membranes of the mitochondria (Figs. 5 and 7B).

The most remarkable characteristic of the subcellular distribution of the RII-B antigenic sites was their association with postsynaptic structures. Independent of the brain region where the specimens were obtained, the immunoreaction product was localized predominantly to postsynaptic structures including somata and their proximal dendrites, distal dendrites found in the neuropil, and dendritic spines (Figs. 5–8), whereas it was rarely observed in myelinated axons. However, the immunoreactivity localized to postsynaptic structures did not display a specificity for any particular type of synapse. For example, the axon terminals in the inferior colliculus containing either round vesicles and forming asymmetric synapses or flattened vesicles and forming symmetric synapses[26] were both apposed by dendrites that were positive for RII-B immunoreactivity (Fig. 8). In addition, the postsynaptic sites were labeled with immunoreaction product in both somata and dendrites (Figs. 5–8). It is important to note that the immunoreaction product in the

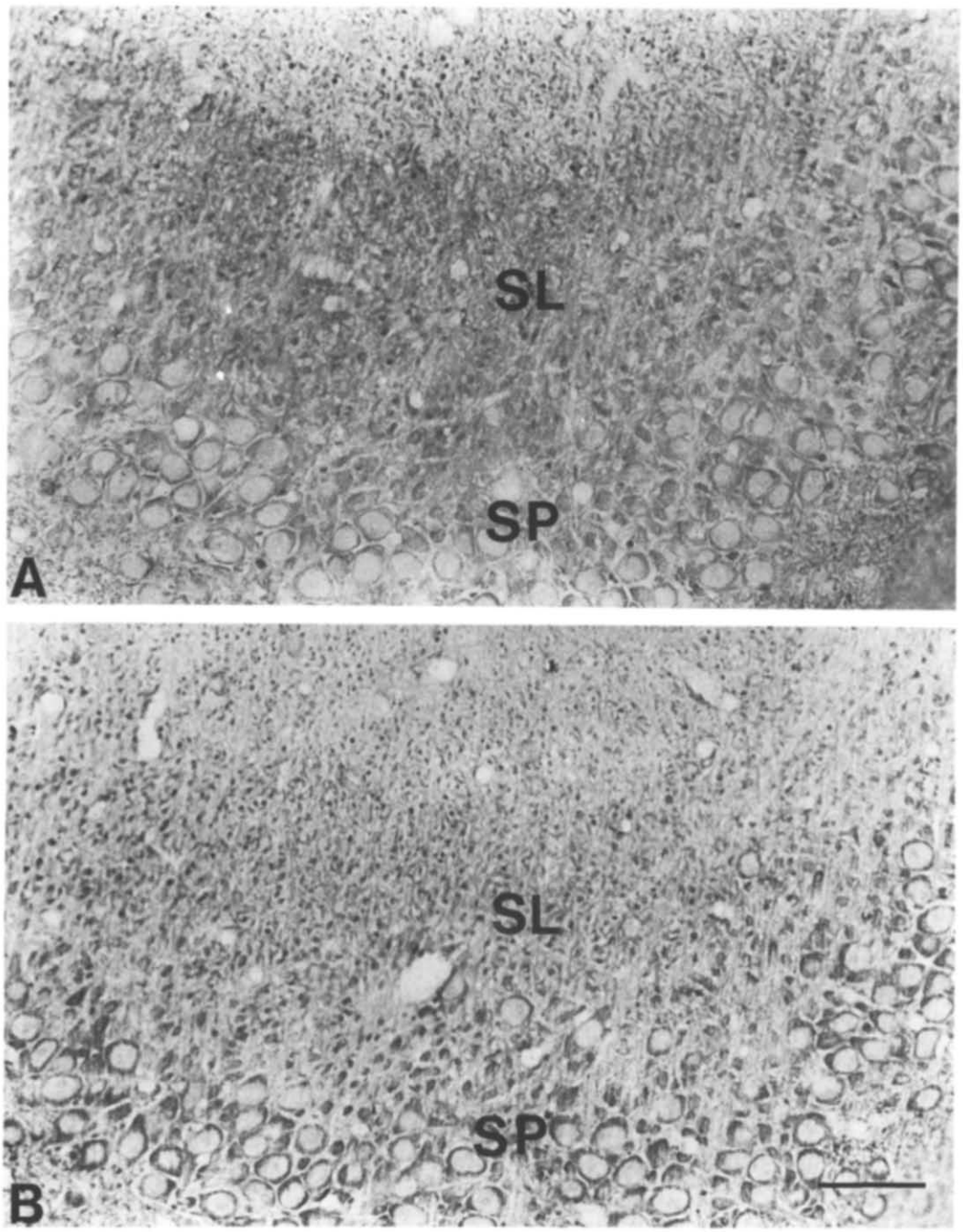

Fig. 4. Photomicrographs of two adjacent sections from the CA3 region of the hippocampus incubated with either RII-B (A) or RII-H (B) antisera. Dense immunostaining occurs in the stratum lucidum (SL), especially in comparison to the superficial dendritic zone (at top of photomicrographs), whereas the stratum pyramidale (SP) displays less dense staining. Note, that RII-B immunostaining is more dense in SL than the RII-H immunostaining. Scale bar for A and B = 50 μm.

dendrites and somata was concentrated not only at the postsynaptic densities, but also at the non-synaptic parts of the membrane and in the adjacent cytoplasm, and appeared frequently as interconnected chains of small granules (Figs. 5–8).

In our experimental conditions axon terminals never displayed RII-B immunoreactivity no matter whether they contained round or flattened vesicles or were apposed to dendrites or somata (Figs. 5–8). This is well reflected in the fact that in the dentate gyrus, a system where the neurons and their processes could be identified, the somata and dendrites of the granule cells displayed RII-B immunoreactivity (Fig. 7B), but their axon terminals, the mossy fibers in the hilus, lacked immunoreaction product (Fig. 7C).

The lack of RII-B immunoreactivity in glial cells was

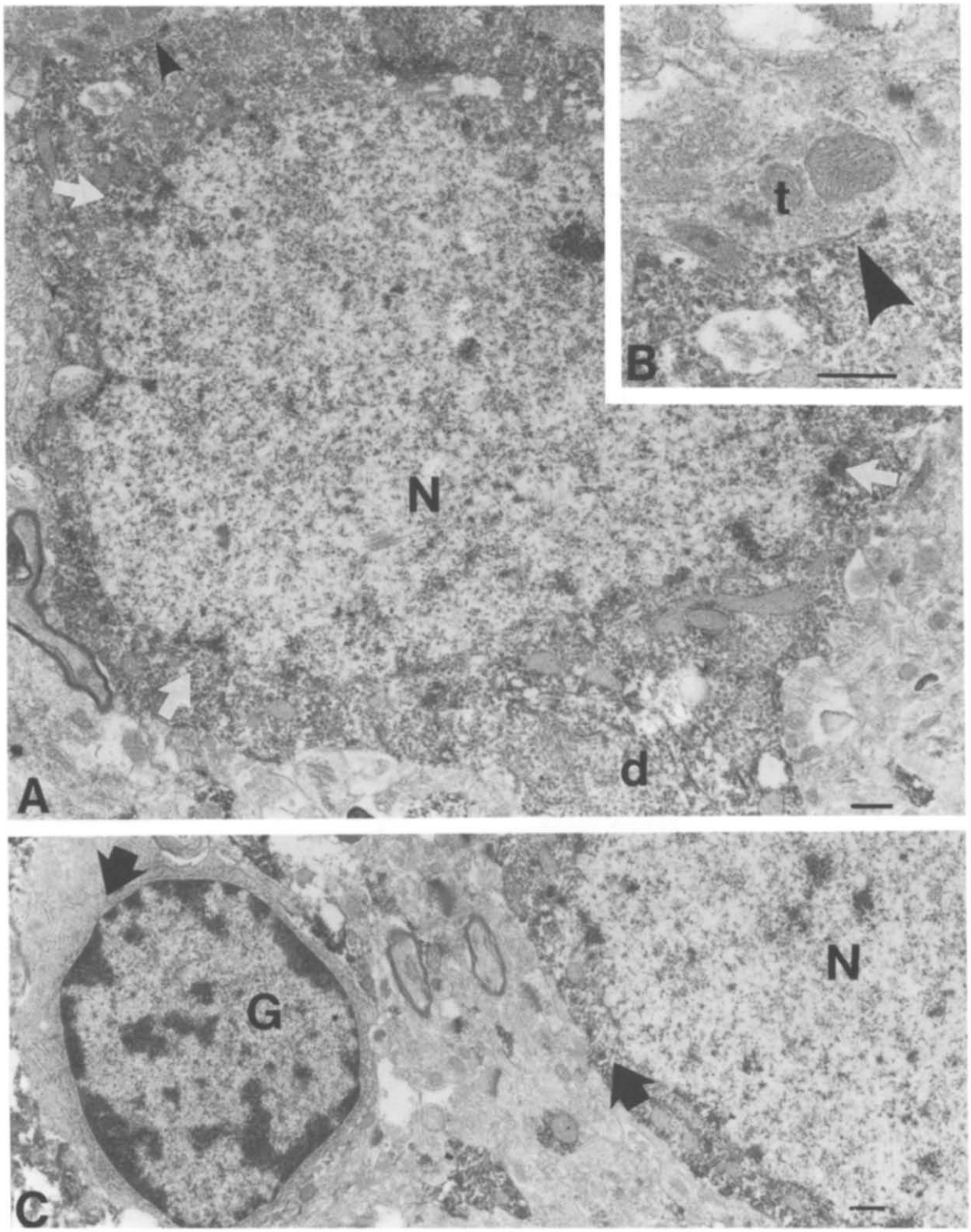

Fig. 5. **Electron micrographs of an RII-B stained preparation obtained from the parietal cortex. A: RII-B positive pyramidal cell.** The immunoreaction product is localized to the perikaryon (white arrows) and the proximal dendrite (d). The nucleus (N) lacks immunostaining. Black arrowhead points to an axo-somatic synapse. B: enlargement of the axo-somatic synapse (arrowhead) from A. An axon terminal (t) forms a symmetric synapse. C shows the difference in staining between the perikaryal cytoplasm (arrowheads) of an unlabeled glial cell (G) and a neuron. The nucleus of the neuron (N) is unstained. Scale bars = 0.5 μm.

clearly indicated by the absence of immunoreaction product in either the cell bodies and processes of astrocytes (Fig. 5C) or in the myelin sheath of myelinated axons (Figs. 6C and 7A). Immunoreaction product was rarely detected within myelinated axons. Also, the endothelial cells surrounding the capillaries displayed no

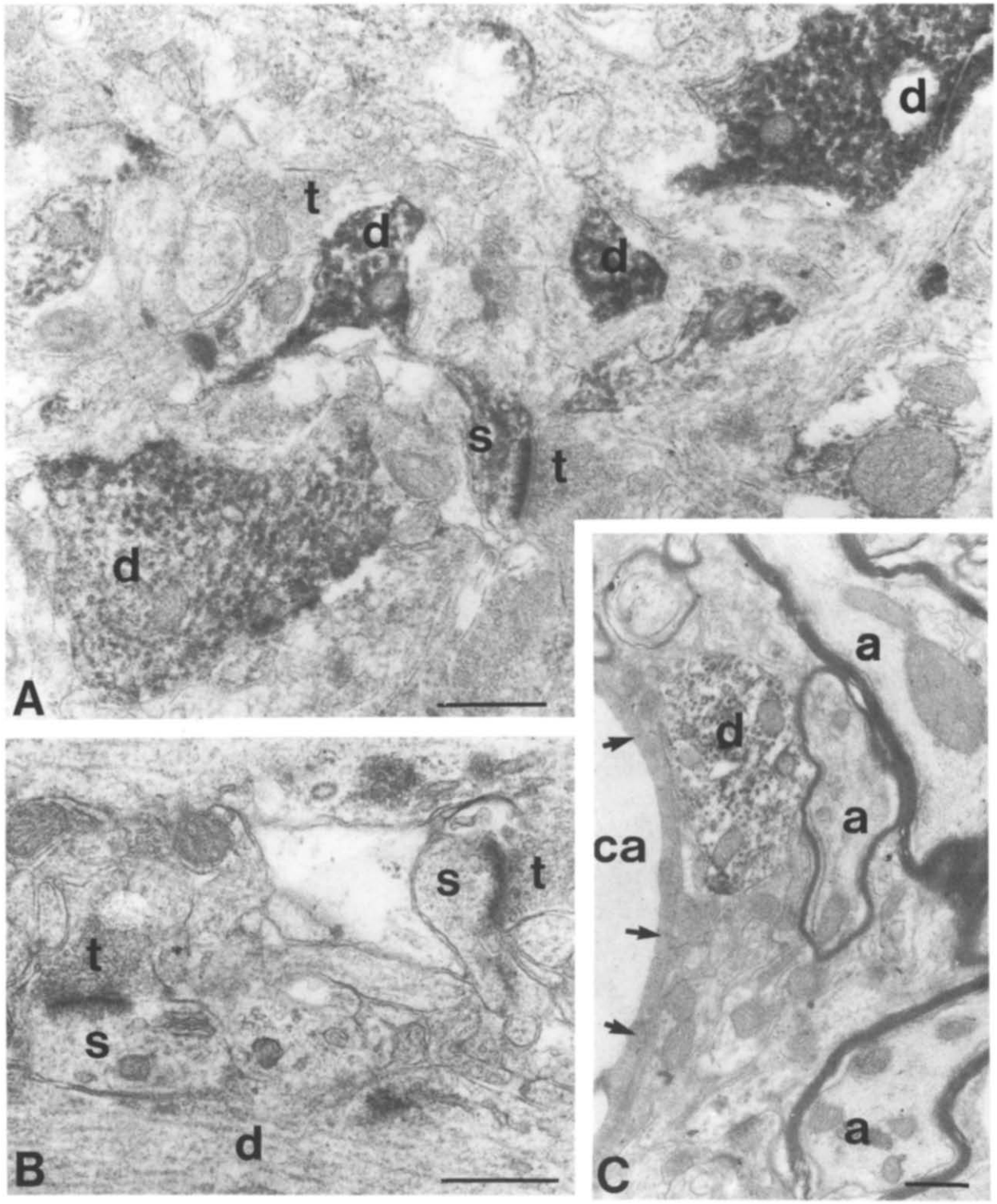

Fig. 6. Electron micrographs of thin sections obtained from two parietal cortex specimens stained with either RII-B antiserum (A and C) or non-immune rabbit serum (B). Note the dense RII-B immunostaining in dendrites (d) and dendritic spines (s) in A, whereas no specific immunoreaction can be found in B. Axon terminals (t) in both A and B do not display immunoreaction product. C: an endothelial cell (arrows) of a capillary (ca) and neighboring myelinated axons (a) lack RII-B immunoreactivity. However, RII-B immunoreaction product is present within a dendrite (d). Scale bars = 0.5 μm.

immunoreaction product (Fig. 6C).

The subcellular distribution of RII-H immunoreactivity showed many similarities with the distribution of RII-B immunostaining. Thus, RII-H immunoreactivity was detected mainly in postsynaptic structures: in neuronal somata and dendrites (Fig. 9C). The cell nuclei

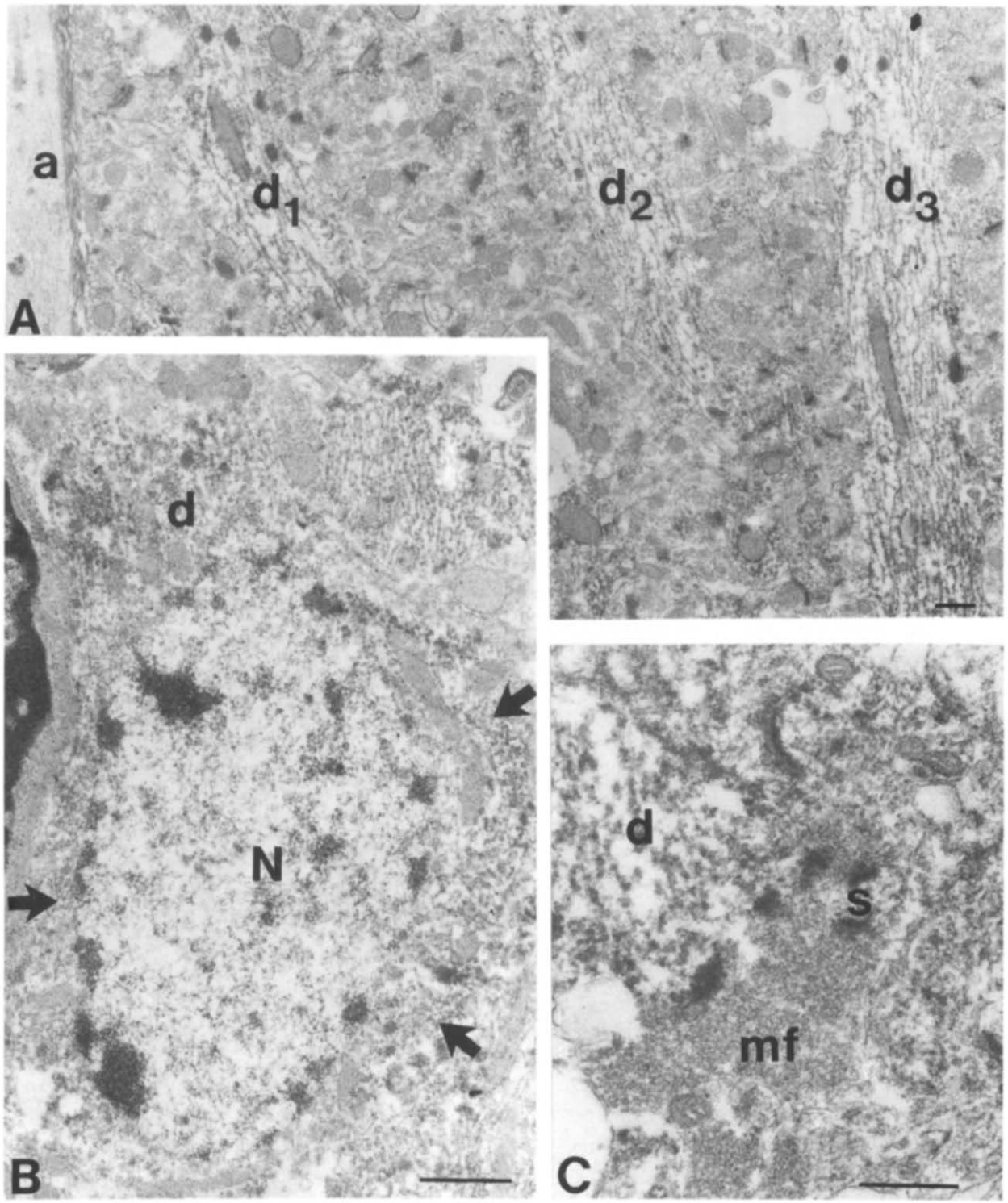

Fig. 7. Electron micrographs of RII-B-stained preparations from the stratum radiatum of CA1 region of the hippocampus (A), stratum granulosum (B) and hilus (C) of the dentate gyrus. Note the immunostained, parallel dendrites (d_1, d_2 and d_3) and the unstained myelinated axon (a) in A. B: a granule cell with immunoreaction product in its perikaryal cytoplasm (arrows) and in its proximal dendrite (d), whereas its nucleus (N) is unstained. C: a terminal of a mossy fiber (mf) that originates from a granule cell, forms a synapse with a dendrite (d) and a dendritic spine (s) of a hilar neuron. Immunoreactivity is localized in the dendrite and spine. Scale bars = 0.5 μm.

lacked this type of immunoreaction product and the endothelial cells were also negative. However, some important differences were also observed. Among these was the occurrence of RII-H immunoreaction product in some glial cell bodies and processes (Fig. 9A). Also, immunoreaction product within myelinated axons was

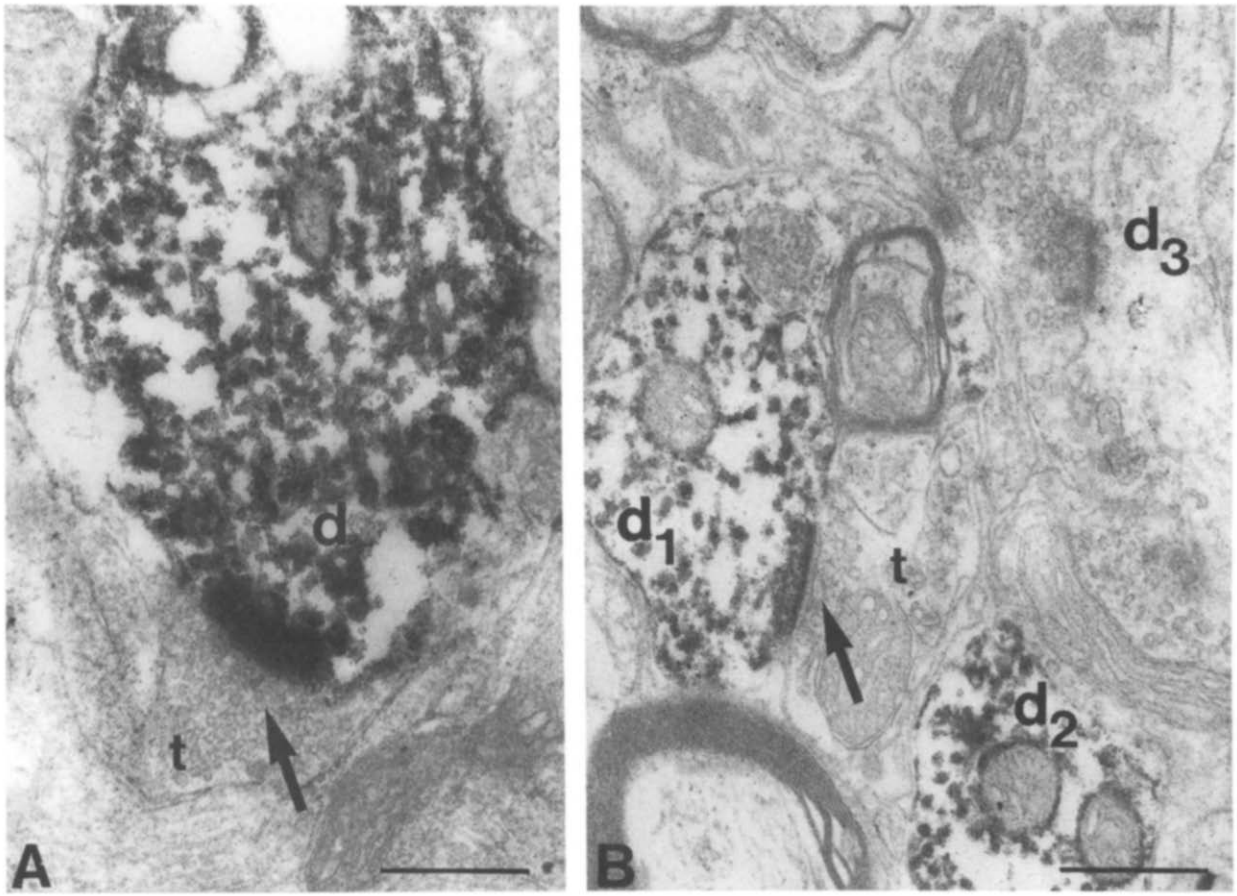

Fig. 8. Electron micrographs of RII-B-stained preparations obtained from the central nucleus of the inferior colliculus. A: an axon terminal (t) that contains round vesicles (arrow) forms an asymmetric synapse with a dendrite (d). B: another axon terminal (t) that contains flattened vesicles (arrow) forms a symmetric synapse with a dendrite (d_1). Note that the immunoreaction product is localized to the dendrites with some association to the postsynaptic densities. In dendrite d_2 the immunoreaction product is apparently not associated with a synaptic density. A dendrite, negative for immunostaining (d_3), is also present. Scale bars = 0.5 μm.

frequently detected (Fig. 9B).

Electron microscopic specimens obtained from sections adjacent to the RII-B or RII-H immunostained sections but incubated with non-immune rabbit serum did not display immunoreaction product (Fig. 6B). This showed that the above-described characteristics of the localization of RII-B or RII-H immunoreaction product reflected specific antigen–antibody binding sites and artifacts were probably not superimposed on the specific immunocytochemical staining patterns.

DISCUSSION

In this study the cellular and subcellular distribution of RII-B, the neural specific regulatory subunit of the type II cAMPdPK and one of the major cAMP-binding proteins, was studied in rat brains. The main data of this combined light and electron microscopic immunocytochemical analysis can be summarized as follows: (1) RII-B antigenic sites occurred in all of the studied brain regions but the regional distribution of the antigenic sites was heterogeneous; (2) RII-B immunoreaction product was predominantly localized to neurons; even though a number of processes in the neuropil at the light microscopic level contained specific immunoreactivity, these were determined to be dendrites in electron microscopic preparations and not glial or endothelial cells; (3) RII-B immunoreactivity was found in all types of neurons, but the amount of immunoreaction product varied from neuron to neuron; (4) RII-B immunoreactivity was concentrated in neuronal somata and dendrites, whereas the nuclei did not contain immunoreaction product; (5) RII-B immunoreactivity rarely occurred in myelinated axons and was never found in axon terminals; and (6) RII-B immunoreaction product was associated with the postsynaptic densities, although it was not specific to any type of synapse and was also found at adjacent non-synaptic sites.

The fact that RII-B immunoreactivity was detected in all the studied brain regions is consistent with the results of recent autoradiographic studies which described [^{3}H]cAMP binding sites throughout the brain[10]. How-

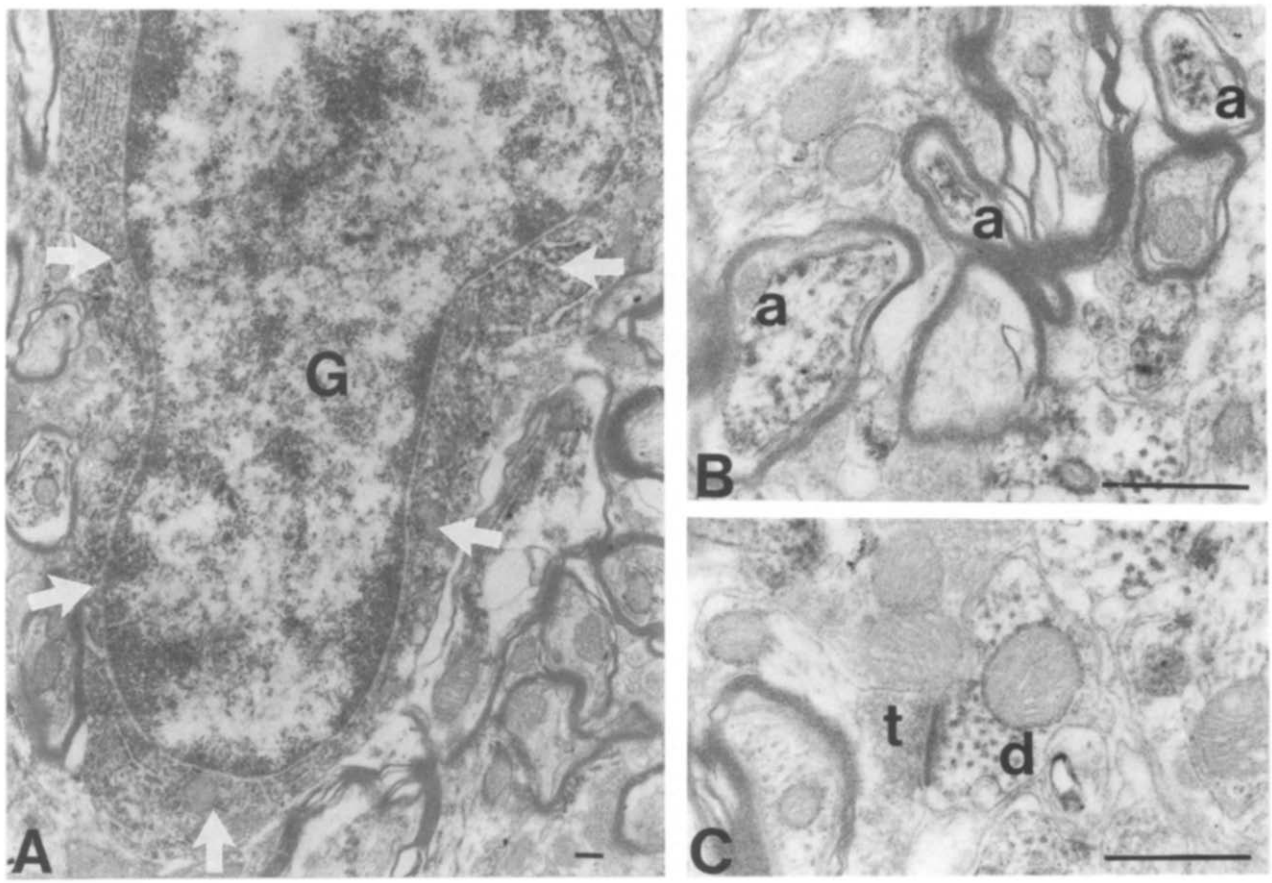

Fig. 9. Electron micrographs of an RII-H stained preparation obtained from the central nucleus of the inferior colliculus. A: a glial cell (G) with RII-H immunoreaction product (white arrows) in its cytoplasm. B: some myelinated axons (a) display RII-H immunostaining. C: an immunostained dendrite (d) forms a synapse with an axon terminal (t) that lacks immunoreaction product. Scale bars = 0.5 μm.

ever, the regional distribution of RII-B immunoreactivity did not match consistently with that of [^{3}H]cAMP binding sites. For example, our results showed that RII-B immunoreactivity in the hippocampus was more concentrated in the dendritic layers than in the cellular layers. In contrast, radioactive labeling with [^{3}H]cAMP to identify all of the cAMP binding proteins showed more intense binding in the cellular layers[10]. This supports the notion that RII-B represents a unique subset of cAMP binding proteins.

In previous studies Western immunoblot data showed that astrocyte membranes also displayed RII-B immunoreactivity[33]. In our experimental conditions, however, RII-B antibodies labeled only neuronal elements; possible antigenic sites in glial elements were below the detectable level. This confirms that RII-B might reflect an adaptation of the type II cAMPdPK to the specialized metabolic and functional roles of neurons[6,32,33,36]. In addition, these data show that the wide variety of effects of cAMP observed in glial cells[15] are probably transduced through cAMP binding proteins other than RII-B, namely RII-H or RI. Consistent with this notion is the observation that RII-H occurred often in glial cells in the present study.

The finding that virtually all neuron types contained RII-B immunoreaction product, regardless of their morphological, neurochemical or electrophysiological characteristics, underscores that RII-B participates in many common intraneuronal processes. However, the remarkable variation among the individual neurons in terms of the accumulation of RII-B immunoreaction product is worth noting. This finding may indicate that different neurons utilize the RII-B-linked molecular machinery to a different extent, depending on their function, and may explain the often contradictory results obtained with externally applied cAMP analogues onto neurons[20,24,30]. In addition, the heterogeneous distribution of RII-B immunostaining in the apical dendrites of CA3 pyramidal cells suggests that certain synapses may require different amounts of RII-B for their function.

The main characteristics of the intraneuronal distribution of RII-B immunoreactivity were basically similar to that of RII-H described in a previous study by De Camilli et al.[5]. Thus, RII-B immunoreactivity was accumulated in the neuronal somata and dendrites and not in nuclei. The lack of detectable levels of RII-B and RII-H immunoreactivity in nuclei supports the current notion

that the regulatory functions of cAMP on gene transcription[9,21] require the presence of only the catalytic subunit of cAMPdPK in the nucleus.

The principal finding of this study is that RII-B is associated with postsynaptic, and not with presynaptic, structures. This is reflected in the fact that RII-B immunoreaction product was accumulated in the neuronal somata, dendrites and dendritic spines, was rarely observed in axons, was never detected in axon terminals and was apparently associated with postsynaptic densities. The less frequent occurrence of RII-B antigenic sites in axons than that of RII-H may also indicate the significance of the concentration of RII-B in postsynaptic elements. These data may provide a morphological basis for the involvement of cAMPdPK in several postsynaptic neural functions, including the regulation of receptors and ion channels, which have been suggested by a number of electrophysiological and biochemical experiments[11,14,20,24].

Acknowledgements. This work was supported by NIH Grants NS-15669 (C.E.R.), GM-44427/01 (J.D.S.) and GM-22792 (C.S.R.). The authors gratefully acknowledge Dr. Phillippe Ciofi and Susan Glantz for helpful discussions during the course of the work, and Margot Brundage and Yashoda Jhurani for photographic and technical assistance with the electron microscopic preparations.

REFERENCES

1 Amaral, D.G., A Golgi study of cell types in the hilar region of the hippocampus in the rat, *J. Comp. Neurol.*, 182 (1978) 851–914.
2 Corbin, J.D., Keely, S.L. and Park, C.R., The distribution and dissociation of cyclic adenosine 3:5-monophosphate-dependent protein kinases in adipose, cardiac and other tissues, *J. Biol. Chem.*, 250 (1975) 218–225.
3 Cumming, R., Koide, Y., Krigman, M.R., Beavo, J.A. and Steiner, A.L., The immunofluorescent localization of regulatory and catalytic subunit of cyclic AMP-dependent protein kinase in neuronal and glial cell types of the central nervous system, *Neuroscience,* 6 (1981) 953–961.
4 De Camilli, P., Immunocytochemistry as a tool in the study of protein phosphorylation in the nervous system. In P. Greengard, R. Paoletti, G.A. Robison and S. Nicosia (Eds.), *Advances in Cyclic Nucleotide and Protein Phosphorylation Research, Vol. 17,* Raven, New York, 1984, pp. 489–499.
5 De Camilli, P., Moretti, M., Donini, S.D., Walter, U. and Lohmann, S.M., Heterogeneous distribution of the cAMP receptor protein RII in the nervous system: evidence for its intracellular accumulation on microtubules, microtubule-organizing centers, and in the area of the Golgi complex, *J. Cell. Biol.,* 103 (1986) 189–203.
6 Erlichman, J., Sarkar, D., Fleischer, N. and Rubin, C.S., Identification of two subclasses of type II cAMP-dependent protein kinases, *J. Biol. Chem.*, 255 (1980) 8179–8184.
7 Faull, R.L.M. and Mehler, W.R., Thalamus. In G. Paxinos (Ed.), *The Rat Nervous System, Vol. 1,* Academic, New York, 1985, pp. 129–168.
8 Gessa, G.L., Krishna, G., Forn, J., Tagliamonte, A. and Brodie, B.B., Behavioral and vegetative effects produced by dibutyryl cyclic AMP injected into different areas of the brain. In P. Greengard and E. Costa (Eds.), *Advances in Biochemical Psychopharmacology, Vol. 3,* Raven, New York, 1970, pp. 371–381.
9 Grove, J.R., Price, D.J., Goodman, H.M. and Avruch, J., Recombinant fragment of protein kinase inhibitor blocks cyclic AMP-dependent gene transcription, *Science,* 238 (1987) 530–533.
10 Gundlach, A.L. and Urosevic, A., Autoradiographic localization of particulate cyclic AMP-dependent protein kinase in mammalian brain using [^{3}H]cyclic AMP: implications for organization of second messenger systems, *Neuroscience,* 29 (1989) 695–714.
11 Heuschneider, G. and Schwartz, R.D., cAMP and forskolin decrease γ-aminobutyric acid-gated chloride flux in rat brain synaptoneurosomes, *Proc. Natl. Acad. Sci. U.S.A.,* 86 (1989) 2938–2942.
12 Hockberger, P.E. and Swandulla, D., Direct ion channel gating: a new function for intracellular messengers, *Cell. Mol. Neurobiol.,* 7 (1987) 229–236.
13 Hopkins, W.F. and Johnston, D., Noradrenergic enhancement of long-term potentiation of mossy fiber synapses in the hippocampus, *J. Neurophysiol.,* 59 (1988) 667–687.
14 Huganir, R.L. and Greengard, P., Regulation of receptor function by protein phosphorylation, *Trends Pharmacol. Sci.,* 8 (1987) 472–477.
15 Kimelberg, H.K., Primary astrocyte cultures — a key to astrocyte function, *Cell. Mol. Neurobiol.,* 3 (1983) 1–16.
16 Kugler, P., The enzyme histochemistry of neurotransmitter metabolism. In F. Beck, W. Hild, W. Kriz, R. Ortmann, J.E. Pauly and T.H. Scheiber (Eds.), *Advances in Anatomy Embryology and Cell Biology, Vol. 111,* Springer, Berlin, 1988, pp. 40–60.
17 Lohmann, S.M. and Walter, U., Regulation of the cellular and subcellular concentrations and distribution of cyclic nucleotide-dependent protein kinases. In P. Greengard and G.A. Robison (Eds.), *Advances in Cyclic Nucleotide and Protein Phosphorylation Research, Vol. 18,* Raven, New York, 1984, pp. 63–117.
18 Ludvig, N. and Moshé, S.L., Cyclic AMP derivatives injected into the inferior colliculus induce audiogenic seizure-like phenomena in normal rats, *Brain Research,* 437 (1987) 193–196.
19 Ludvig, N. and Moshé, S.L., Different behavioral and electrographic effects of acoustic stimulation and dibutyryl cyclic AMP injection into the inferior colliculus in normal and in genetically epilepsy-prone rats, *Epilepsy Res.,* 3 (1989) 185–190.
20 Madison, D.V. and Nicoll, R.A., Noradrenaline blocks accommodation of pyramidal cell discharge in the hippocampus, *Nature (Lond.),* 299 (1982) 636–638.
21 Montminy, M.R., Sevarino, K.A., Wagner, J.A., Mandel, G. and Goodman, R.H., Identification of a cyclic-AMP-responsive element within the rat somatostatin gene, *Proc. Natl. Acad. Sci. U.S.A.,* 83 (1986) 6682–6686.
22 Nairn, A.C., Hemmings, H.C. and Greengard, P., Protein kinases in the brain, *Ann. Rev. Biochem.,* 54 (1985) 931–976.
23 Nestler, E.J. and Greengard, P., *Protein Phosphorylation in the Nervous System,* Wiley, New York, 1984, pp. 1–11.
24 Nicoll, R.A., The coupling of neurotransmitter receptors to ion channels in the brain, *Science,* 241 (1988) 545–551.
25 Peters, A., Miller, M. and Kimerer, L.M., Cholecystokinin-like immunoreactive neurons in rat cerebral cortex, *Neuroscience,* 8 (1983) 431–448.
26 Ribak, C.E. and Roberts, R.C., The ultrastructure of the central nucleus of the inferior colliculus of the Sprague–Dawley rat, *J. Neurocytol.,* 15 (1986) 421–438.
27 Roberts, R.C. and Ribak, C.E., An electron microscopic study of GABAergic neurons and terminals in the central nucleus of the inferior colliculus of the rat, *J. Neurocytol.,* 16 (1987) 333–345.
28 Scott, J.D., Glaccum, M.B., Fischer, E.H. and Krebs, E.G.,

Primary-structure requirements for inhibition by the heat-stable inhibitor of the cAMP-dependent protein kinase, *Proc. Natl. Acad. Sci. U.S.A.*, 83 (1986) 1613–1616.

29 Scott, J.D., Glaccum, M.B., Zoller, M.J., Uhler, M.D., Helfman, D.M., McKnight, G.S. and Krebs, E.G., The molecular cloning of a type II regulatory subunit of the cAMP-dependent protein kinase from rat skeletal muscle and mouse brain, *Proc. Natl. Acad. Sci. U.S.A.*, 84 (1987) 5192–5196.

30 Segal, M. and Bloom, F.E., The action of norepinephrine in the rat hippocampus. I. Iontophoretic studies, *Brain Research*, 72 (1974) 79–97.

31 Seress, L. and Ribak, C.E., GABAergic cells in the dentate gyrus appear to be local circuit and projection neurons, *Exp. Brain Res.*, 50 (1983) 173–182.

32 Stein, J.C. and Rubin, C.S., Isolation and sequence of a tryptic peptide containing the autophosphorylation site of the regulatory subunit of bovine brain protein kinase II, *J. Biol. Chem.*, 260 (1985) 10991–10995.

33 Stein, J.C., Farooq, M., Norton, W.T. and Rubin, C.S., Differential expression of isoforms of the regulatory subunit of type II cAMP-dependent protein kinase in rat neurons, astrocytes and oligodendrocytes, *J. Biol. Chem.*, 262 (1987) 3002–3006.

34 Walter, U., Kanof, P., Schulman, H. and Greengard, P., Adenosine 3:5-monophosphate receptor proteins in mammalian brain, *J. Biol. Chem.*, 253 (1978) 6275–6280.

35 Walter, U., Lohmann, S.M., Sieghart, W. and Greengard, P., Identification of the cyclic AMP-dependent protein kinase responsible for endogenous phosphorylation of substrate proteins in synaptic membrane fraction from rat brain, *J. Biol. Chem.*, 254 (1979) 12235–12239.

36 Weldon, S.L., Mumby, M.C. and Taylor, S.S., The regulatory subunit of neural cAMP-dependent protein kinase II represents a unique gene product, *J. Biol. Chem.*, 260 (1985) 6440–6448.